第 32 卷第 12 期 无 机 化 学 学 报 Vol.32 No.12
2016 年 12 月 CHINESE JOURNAL OF INORGANIC CHEMISTRY 2198-2204

三个双肼桥连金属配合物的合成,结构和磁性

李 欢[1] 陈云舟[1] 王艳君[1] 陈云峰[1] 王炳武*,[2] 贾丽慧*,[1]
([1]武汉工程大学化学与环境工程学院,绿色化工过程省部共建教育部重点实验室,武汉 430073)
([2]北京大学化学与分子工程学院,北京分子科学国家实验室,稀土材料化学及应用国家重点实验室,北京 100871)

摘要: 采用水热合成方法得到 3 个新的双肼桥连过渡金属化合物:$[M(N_2H_4)_2Cl_2]_n$ (M=Mn(**1**), Ni(**2**)), $\{[Co_{1.5}(N_2H_4)_3PO_4(H_2O)]\cdot H_2O\}_n$ (**3**),用单晶 X 射线衍射方法对其晶体结构进行表征。化合物 **1** 是以 2 个肼分子桥联金属 Mn 和 Ni 形成 1D 链状结构,而粉末 XRD 显示 **1** 与 **2** 是同构的。化合物 **3** 是以 2 个肼分子桥联金属 Co 形成 1D 链,不同的 1D 链再通过磷酸根 PO_4^{3-}进一步堆积形成 3D 结构。磁性测试表明肼桥在磁性中心之间传递反铁磁耦合作用。

关键词: 肼; 肼桥连配体; 反铁磁交换作用
中图分类号: O614.7+11; O614.81+3; O614.81+2 **文献标识码**: A **文章编号**: 1001-4861(2016)12-2198-07
DOI:10.11862/CJIC.2016.250

Syntheses, Structures and Magnetic Studies of Three Double Hydrazine Bridging Transition Metal Compounds

LI Huan[1] CHEN Yun-Zhou[1] WANG Yan-Jun[1] CHEN Yun-Feng[1] WANG Bing-Wu*,[2] JIA Li-Hui*,[1]
([1]*Key Laboratory for Green Chemical Process of Ministry of Education, School of Chemistry and Environmental Engineering, Wuhan Institute of Technology, Wuhan*, 430074, *China*)
([2]*Beijing National Laboratory for Molecular Science, The State Key Laboratory of Rare Earth Materials Chemistry and Applications, College of Chemistry and Molecular Engineering, Peking University, Beijing* 100871, *China*)

Abstract: By employing the hydrothermal method, we have synthesized three transition metal compounds with double hydrazine (N_2H_4) as bridge: $[M(N_2H_4)_2Cl_2]_n$(M=Mn(**1**), Ni(**2**)), $\{[Co_{1.5}(N_2H_4)_3PO_4(H_2O)]\cdot H_2O\}_n$(**3**). Single-crystal X-ray diffraction reveals that the compound **1** are one-dimensional (1D) chains with two hydrazine molecules as bridge ligands. And powder X-ray diffraction analysis reveals that compounds **1** and **2** are isomorphous. The compound **3** first form 1D chains through two hydrazine molecules as bridge ligands and the PO_4^{3-} connect the chains into a 3D extended structure. The magnetic measurement reveals the hydrazine as bridge ligand can mediate the antiferromagnetic (AF) coupling interaction between magnetic centers. CCDC: 1503462, **1**; 1503463, **3**.

Keywords: hydrazine; hydrazine bridge ligand; antiferromagnetic interaction

0 Introduction

In molecule-based magnetic materials, transition-metal compounds with short bridge ligand of one- to three-atom, such as O^{2-}, CN^-, N_3^-, $HCOO^-$, and $C_2O_4^{2-}$ are under intense investigation[1-2]. As a short two-atom bridge ligand, the ability of unsubstituted hydrazine (N_2H_4) to mediate magnetic coupling was scarcely

收稿日期:2016-07-02。收修改稿日期:2016-09-14。
国家自然科学基金(No.21101123,21441007)和武汉工程大学研究生创新基金(No.CX2015160)资助项目。
*通信联系人。E-mail: jialihui715@wit.edu.cn; bwwang@pku.edu.cn

investigated. In our previous work[3-5], we have already learned that hydrazine mediate AF coupling when it act as co-ligand. We also found that sulfate can bridge Co^{2+} and Ni^{2+} ions and construct weak ferromagnets with hydrazine as its co-ligand. The mixed sulfate and hydrazine bridges of the weak ferromagnets prevent any detailed investigation of the ability of hydrazine to mediate magnetic coupling. More effort was here placed into synthesizing transition metal compounds containing solo hydrazine bridges. Here we have obtained three transition metal compounds containing hydrazine, two of them are 1D chain compounds containing double hydrazine bridges $[M(N_2H_4)_2Cl_2]_n$ (M= Mn (**1**), Ni (**2**)), the other is 3D framework compound containing double hydrazine bridges $\{[Co_{1.5}(N_2H_4)_3PO_4(H_2O)]\cdot H_2O\}_n$. We studied the ability of hydrazine to mediate magnetic coupling and how it was affected by the structure of compounds and the anisotropy of the magnetic centers.

1 Experimental

All starting materials were commercially available at analytical grade and used as purchased without further purification. $MnCl_2\cdot H_2O$ (≥99%, AR), $NiCl_2$ (≥99%, AR), $Co(NO_3)_2\cdot 6H_2O$ (≥99%, AR), N_2H_4 (85%), HCl (36.5%), HPF_6 (≥60%, AR).

1.1 Preparations of compounds 1~3

Preparations of **1**: $MnCl_2\cdot H_2O$ 1 mL (1 $mol\cdot L^{-1}$ water solution), HCl 1 mL (1 $mol\cdot L^{-1}$), H_2O 8 mL, N_2H_4 2 mL and 2 drops of C_2H_5OH were added to glass bottle, then the mixture was heated at 90 ℃ for 2 days in a furnace and naturally cooled to obtain the colorless needle-like crystals. The crystals were washed by water and dried in the air. Yield based on $MnCl_2$: 65%. Elemental analysis Calcd. for $MnN_4H_8Cl_2$ (%): N 29.49, H 4.21; Found(%): N 29.46, H 4.24.

Preparations of **2**: 5 mL N_2H_4 was added to 10 mL $NiCl_2$ water solution of 0.02 $mol\cdot L^{-1}$, at the speed of 1 $mL\cdot h^{-1}$, stirring while adding. Then we got light blue powder. Yield based on $NiCl_2$: 85%. Elemental analysis Calcd. for $NiN_4H_8Cl_2$ (%): N 28.91, H 4.13; Found(%): N 28.88, H 4.15.

Preparation of **3**: $Co(NO_3)_2\cdot 6H_2O$ 1mL (1 $mol\cdot L^{-1}$), $N_2H_4\cdot H_2O$ 4 mL, HPF_6 0.25 μL and H_2O 5 mL were added to a 25 mL Teflon-lined stainless-steel autoclave in sequence, then the mixture was heated at 90 ℃ for **2** days in a furnace and naturally cooled to obtain the orange needle crystals and yellow microlite. The orange needle crystals were picked out, and washed by water and dried in the air. Yield based on Co $(NO_3)_2$: 6.3% . Elemental analysis Calcd. for $Co_{1.5}N_6H_{16}O_6P$ (%): N 26.63, H 5.11; Found (%): N 26.01 ,H 5.02.

1.2 X-ray crystallography and physical measurements

The crystallographic data for the single crystal of compounds **1** or **3** was collected at 293 K on an Agilent Technology SuperNova Atlas Dual System with a Cu microfocus source and focusing multilayer optics using radiation Cu $K\alpha$ (λ=0.071 073 nm) Empirical absorption corrections were applied using the CrysAlisPro program[6-7]. The structure was solved by the direct method and refined by full matrix least-squares on F^2 using SHELXL-97[8-9]. All the non-hydrogen atoms were refined using anisotropic thermal parameters. Hydrogen atoms were located geometrically and refined in riding mode. The detailed crystallographic parameters of **1** and **3** are listed in Table 1, and selected bond lengths and angles are listed in Table 2.

CCDC: 1503462, **1**; 1503463, **3**.

Table 1　Crystallographic data for compounds 1 and 3

Compound	**1**	**3**
Empirical formula	$H_8Cl_2MnN_4$	$H_{16}Co_{1.5}N_6O_6P$
Formula weight	189.9	315.55
Crystal system	Monoclinic	Monoclinic
Space group	*I*2/*m*	$P2_1/c$
a / nm	0.429 37(9)	0.864 75(17)

Continued Table 1

b / nm	0.804 27(16)	0.929 94(19)
c / nm	0.994 5(2)	1.208 7(2)
β / (°)	101.74(3)	108.06(3)
V / nm^3	0.336 24(12)	0.924 11(30)
Z	2	4
D_c / (g·cm^{-3})	1.876	1.811
μ / mm^{-1}	2.653	2.921
θ range / (°)	4.19~27.06	3.64~27.52
Final R indices [$I \geqslant 2\sigma(I)$]	R_1=0.030 1, wR_2=0.066 9	R_1=0.028 9, wR_2=0.060 1
R indices (all data)	R_1=0.040 8, wR_2=0.063 9	R_1=0.048 7, wR_2=0.063 2
Goodness of fit	1.008	0.931
$(\Delta\rho)_{max}$, $(\Delta\rho)_{min}$ / (e·nm^{-3})	303, −372	331, −502

Table 2 Selected bond lengths (nm) and bond angles (°) for compounds 1 and 3

1					
Mn-N1	0.229 0(2)	Mn-N1	0.229 0(2)	Mn-N1	0.229 0(2)
Mn-N1	0.229 0(2)	Mn-Cl	0.282 48(12)	Mn-Cl	0.282 48(12)
N1-N1	0.149 8(4)				
N1-Mn-N1	91.92(13)	N1-Mn-N1	180.00(9)	N1-Mn-N1	88.08(13)
N1-Mn-N1	88.08(13)	N1-Mn-N1	180.000(1)	N1-Mn-N1	91.92(13)
N1-Mn-Cl	86.12(7)	N1-Mn-Cl	93.88(7)	N1-Mn-Cl	93.88(7)
N1-Mn-Cl	86.12(7)	N1-Mn-Cl	93.88(7)	N1-Mn-Cl	86.12(7)
N1-Mn-Cl	86.12(7)	N1-Mn-Cl	93.88(7)	N1-Mn-Cl	93.88(7)
Cl-Mn-Cl	180.0	N1-N1-Mn	112.97(17)		
3					
Co1-N1	0.217 2(2)	Co1-N1	0.217 2(2)	Co1-N3	0.218 4(2)
Co1-N3	0.218 4(2)	Co2-O1	0.209 29(17)	Co2-N2	0.215 8(2)
Co2-N4	0.215 9(2)	Co2-O4	0.216 60(17)	Co2-N5	0.218 1(2)
Co2-N6	0.222 1(2)	P-O1	0.153 61(17)	P-O3	0.154 0(2)
P-O2	0.155 00(18)	P-O4	0.155 35(18)	N4-N3	0.146 4(3)
N2-N1	0.145 7(3)	N6-N5	0.145 7(3)	N5-Co2	0.218 1(2)
O1-Co2	0.209 29(17)				
O1S-Co1-O1S	180.00(8)	O1S-Co1-N1	88.06(8)	O1S-Co1-N1	91.94(8)
O1S-Co1-N1	91.94(8)	O1S-Co1-N1	88.06(8)	N1-Co1-N1	180.0
O1S-Co1-N3	90.96(8)	O1S-Co1-N3	89.04(8)	N1-Co1-N3	88.94(8)
N1-Co1-N3	91.06(8)	O1S-Co1-N3	89.04(8)	O1S-Co1-N3	90.96(8)
N1-Co1-N3	91.06(8)	N1-Co1-N3	88.94(8)	N3-Co1-N3	180.0
O1-Co2-N2	86.83(8)	O1-Co2-N4	93.41(7)	N2-Co2-N4	92.13(8)
O1-Co2-O4	178.18(7)	N2-Co2-O4	92.86(8)	N4-Co2-O4	88.39(7)
O1-Co2-N5	89.74(8)	N2-Co2-N5	91.49(8)	N4-Co2-N5	175.32(8)
O4-Co2-N5	88.48(8)	O1-Co2-N6	90.54(8)	N2-Co2-N6	175.26(8)
N4-Co2-N6	91.95(8)	O4-Co2-N6	89.65(8)	N5-Co2-N6	84.55(8)
O1-P-O3	111.18(10)	O1-P-O2	109.13(10)	O3-P-O2	108.93(10)

Continued Table 2

O1-P-O4	109.70(10)	O3-P-O4	109.35(10)	O2-P-O4	108.50(10)
P-O4-Co2	138.10(10)	N3-N4-Co2	120.05(15)	N4-N3-Co1	118.88(15)
N1-N2-Co2	118.93(14)	N5-N6-Co2	115.98(15)	N6-N5-Co2	114.79(15)
N2-N1-Co1	120.96(15)	P-O1-Co2	140.35(11)		

PXRD data for compounds **1**~**3** were collected in the range of 5°~50° for 2θ on crystalline samples using a Rigaku Dmax 2000 diffractometer with Cu $K\alpha$ radiation (λ=0.154 18 nm, 40 kV, 40 mA) in flat-plate geometry, at room temperature. The experimental powder X-ray diffraction pattern was compared to the calculated one from the single-crystal structure to identify the phase of the sample in the Fig.S1~S2 (Supporting information).

Elemental analysis of nitrogen and hydrogen was performed using an Elementar Vario EL analyzer. The FTIR spectra were recorded against pure crystal samples in the range of 4 000~600 cm^{-1} using a Nicolet iN10 MX Microinfrared Spectrometer. (Fig.S3 in Supporting Information)

Magnetic measurements were performed on a MPMS XL-5 SQUID (Superconductivity Quantum Interference Device) magnetometer with crystalline samples fixed in a white capsule by parafilm or eicosane. Diamagnetic corrections were estimated by using Pascal constants[10] and background corrections by experimental measurements on sample holders.

2 Results and discussion

2.1 Synthesis

Hydrothermal reaction is a convenient and effective route to obtain high-quality single crystals[11-12]. For compound **1**, its really hard to obtain good crystal for measurement because the 1D chain compounds are always needle-like crystals which is easy to be twin crystal. So we managed to do many experiments to look for the optimal reaction conditions through adjusting the hydrothermal temperature, pH value and solvent. For compound **3**, it is got by accident. We were trying to get another compound, which is 1D chain compound containing hydrazine bridge and counter ion PF_6^-, but compound 3 was got by accident due to the oxidation of phosphorus and the PF_6^- were changed to the PO_4^{3-} under the hydrothermal condition.

2.2 Crystal structures

Powder X-ray diffraction analysis reveals that compounds **1** and **2** are isomorphous (Fig.S1). Compound **1** crystallizes in monoclinic crystal system, *I*2/*m* space group. Single-crystal X-ray diffraction reveals that **1** has a chain structure, and the repeating unit is $[M(N_2H_4)_2Cl_2]$, while no lattice water in the crystal. Mn^{2+} ions locate in an octahedron coordination environment (Fig.1a), the octahedral Mn^{2+} ions are surrounded by four equatorial N atoms from four different hydrazine molecules and two Cl^- atoms in the axial direction, which also act as counter ions. The angles of *cis* O-M-O ranges from 86.18° to 93.81°, while all the *trans* angles are 180°. Comparing with the reported compounds containing a monodentate hydrazine and the uncoordinated hydrazine (N-N 0.146 0 nm)[13-14], the distance between the two nitrogen atoms (0.150 62 nm) for **1** is slightly longer but the angle of M-N-N (113.34°) for **1** is a bit smaller than those of reported compounds. This longer

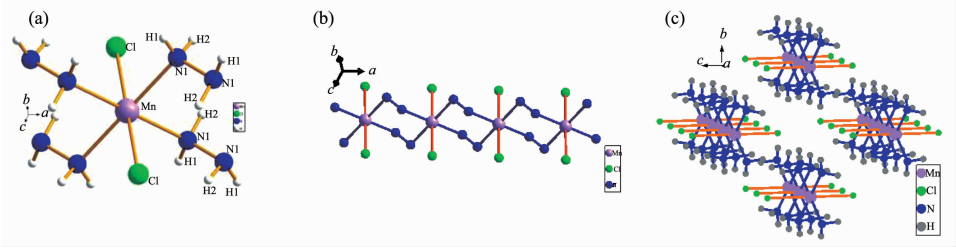

Fig.1 Geometry structure of compound **1** (a) Coordination environment of Mn^{2+} in **1**; (b) 1D chain of **1**; (c) 3D framework of **1**

distance and smaller angel in hydrazine molecule can be probably attributed to its coordination mode as bidentate ligand.

The hydrazine molecules connect the neighboring Mn^{2+} centers through a *syn-syn* coordination mode and form a 1D chain structure along *a*-axis (Fig.1b), the intra-chain distance between the adjacent Mn^{2+} ions is 0.429 nm. The 3D packing structure is shown in Fig. 1c, the distance between the chains is 0.641 6 nm.

Single-crystal X-ray diffraction reveals that **3** crystallizes in the monoclinic system, $P2_1/c$ space group and the repeating unit is $[Co_{1.5}(N_2H_4)_3PO_4(H_2O)]\cdot H_2O$. The main structure of **3** is a 3D neutral network involving Co^{2+} centers connected by hydrazine molecules N_2H_4 and phosphate anions PO_4^{3-} bridges (Fig.2). As shown in Fig.2a, each Co^{2+} ion resides at an inversion center and is six-coordinated in a distorted octahedral configuration, which includes four N atoms from four different hydrazine bridges in the equatorial plane and two O atoms from two PO_4^{3-} anions or from two H_2O molecules in the axis direction. The *cis*-angles of O-Co-O range from 84.55° to 93.41° (Table 2) and the *trans*-angle is from 175.26° to 180°. Different from 1D compound **1**, the N-N bond distance for **3** are 0.145 7(3) and 0.146 4(3) nm, and the angle of Co -N-N ranges from 114.79(15)° to 120.96(15)°. The N-N bond distance and the angle for **3** in the hydrazine bridging ligand are similar to the former ones[4,13,15].

Similar to our previous 3D compounds containing hydrazine[4], the structures of **3** can be regarded as the hydrazine bridged 1D chain Co-N_2H_4-Co which are connected into 3D framework by phosphate anions (Fig.2b, 2c). The hydrazine molecules act as a *trans*-bridging bidentate ligands and link the adjacent Co^{2+} metal ions into the 1D infinite chains, with the Co⋯Co distance 0.426 nm. All these 1D chains are parallel to the *ab* plane, and run along two directions alternately: the *a*, *b* direction and *a*, −*b* direction. Here phosphate anions act as bidentate mode to bridge the two Co^{2+} metal ions from different two 1D chains and so every PO_4^{3-} anion links two chains, one is with a, b direction and the other is with a, -b direction. The bridging PO_4^{3-} anions are above and below the layer alternatively. The adjacent distance of Co⋯Co bridged by PO_4^{3-} is 0.619 nm. Every 1D chain is connected further with other chains by PO_4^{3-} anions to generate a 3D structure.

2.3 Magnetic property

Magnetic measurements were carried out on solid samples of compounds **1**~**3** According to the magnetic data, it was suggested dominant antiferromagnetic coupling interactions between the M^{2+} ions in all three compounds. Although compounds **1**, **2** are 1D structure and compound **3** is 3D structure, the magnetic properties of the three compounds are similar due to their isomorphic structures with double hydrazine bridge.

The $\chi_M T$ values increase sharply in the low temperature range and then smoothly in higher temperature and reach 4.47 $cm^3\cdot mol^{-1}\cdot K$ (**1**), 1.22 $cm^3\cdot mol^{-1}\cdot K$ (**2**) and 4.28 $cm^3\cdot mol^{-1}\cdot K$ (**3**) at room temperature (Fig.3a), the $\chi_M T$ values of **1**~**2** are as expected for the isolated divalent metal ions[16], but the $\chi_M T$ value of **3** is significantly larger than the spin-only value 1.875 $cm^3\cdot mol^{-1}\cdot K$ for S=3/2,which is close to the experimental values reported for other Co^{2+} compounds[15,17]. The magnetic susceptibilities χ_M for

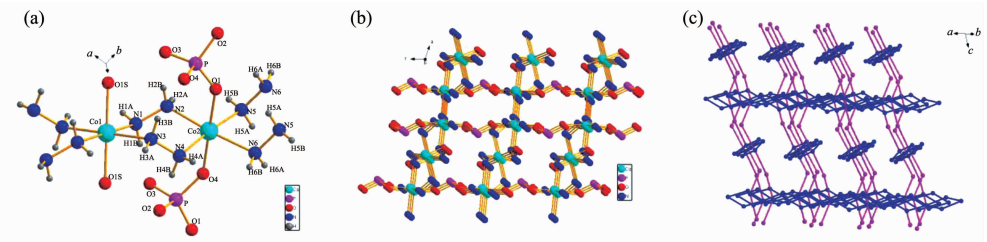

Fig.2 (a) Coordination environments of the metal ion and ligands for **3**; (b) Perspective view of the 3D framework structure of **3** viewed along the *b* axis; (c) Schematic view of the 3D network structure of **3** with phosphate (PO_4^{3-}) represented by P atom and H atom omitted

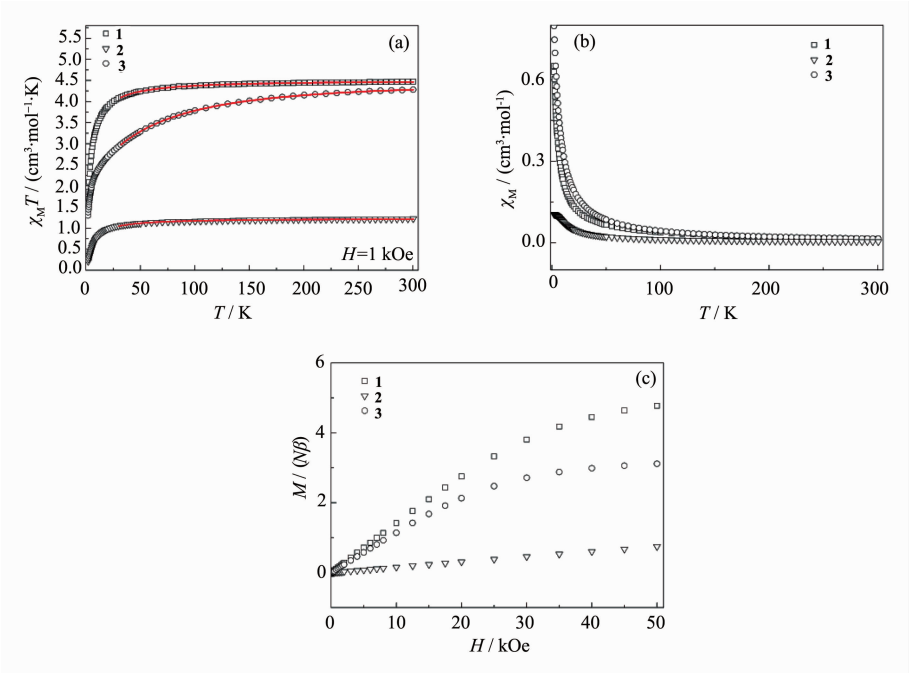

Fig.3　(a) Temperature dependence of $\chi_M T$ of **1**~**3** with solid lines being fitted results; (b) Temperature dependence of χ_M of **1**~**3**; (c) Field dependence of M of **1**~**3**

compounds **1**~**3** in a field of 1 kOe obey Curie-Weiss law $\chi_M = C/(T-\theta)$ (Fig.3b) with the Curie constant C= 4.54 $cm^3 \cdot mol^{-1} \cdot K$ (**1**), 1.24 $cm^3 \cdot mol^{-1} \cdot K$ (**2**) and 4.71 $cm^3 \cdot mol^{-1} \cdot K$ (**3**), negative Weiss constants θ of −3.29 K (**1**), −6.04 K (**2**) and −22.8 K (**3**). The negative Weiss constant indicate the overall AF coupling in compounds **1**~**3**. The field dependence of the magnetization of **1**~**3** measured at 2 K increase linearly (Fig. 3c). At 2 K, the magnetization at 50 kOe reach 4.77$N\beta$ for **1**, 0.74$N\beta$ for **2** and **3**. $N\beta$ for **3**, approaching to saturation magnetization values of *ca.* 5$N\beta$, 2$N\beta$ and 3$N\beta$ expected for one isolated spin S= 5/2, S =3/2 and S =1, which indicated that the AF coupling was weak.

Considering the 1D equally spaced chain structures, the $\chi_M T$ value of **1** can be fitted by Fisher′s 1D Heisenberg chain model[18-20] (S=5/2 and S=3/2, $H=-2JS_iS_j$) expressed by the following equation:

$$\chi_{chain} = \frac{Ng^2\beta^2 S(S+1)}{3kT}\frac{1+u}{1-u} \qquad (1)$$

where $u = \coth\left[\frac{2JS(S+1)}{kT}\right] - \frac{kT}{2JS(S+1)}$. J is the coupling constant of the neighboring M^{2+} bridged by N_2H_4. N, g, β, k and T have their usual meanings.

The $\chi_M T$ value of **2** also can be fitted with the following analytical expression for an antiferromagnetic chain of S=1 with the Hamiltonian $H=-2JS_iS_j$[18,21]:

$$\chi_{chain} = \frac{Ng^2\beta^2}{kT}\frac{2.0+0.019\,4x+0.777x^2}{3.0+4.346x+3.232x^2+5.834x^3} \qquad (2)$$

where $x = |2J|/(kT)$. J is the coupling constant of the neighboring Ni^{2+} bridged by N_2H_4. N, g, β, k and T have their usual meanings.

The best fitting parameters are J=0.37 cm^{-1}, g= 2.03, and R=4.46×10^{-4} for **1** (R is defined as $\Sigma[(\chi_M T)_{obsd} - (\chi_M T)_{calc}]^2/\Sigma[(\chi_M T)_{obsd}]^2$). For **2**, the corresponding fitting parameters are J=1.22 cm^{-1}, g=2.22, and R =1.37 × 10^{-4}.

As for **3**, the weak antiferromagnetic coupling is likely to mediate through the hydrazine chains (-Co-N_2H_4-)$_n$. However, it is too weak to show up against spin-orbit coupling due to the small anisotropic pseudo-spins of cobalt(Ⅱ) ion (S=1/2 under 30 K)[10,18], which led to unsatisfactory accordance with Fisher′s 1D Heisenberg chain model. In order to get an estimate of the strength of the antiferromagnetic exchange interaction, a simple phenomenological equation can be used[22]:

$$\chi T = A\exp[-E_1/(kT)]+B\exp[-E_2/(kT)] \quad (3)$$

where $A+B$ equals Curie constant, and E_1, E_2 represent the activation energies corresponding to the spin-orbit coupling and the antiferromagnetic exchange interaction. The value found for Curie constant ($C=A+B$) above 15 K is 4.62 $cm^3 \cdot mol^{-1} \cdot K$, which agrees well with that obtained from the Curie-Weiss law in the high temperature range. Moreover, the value found for the antiferromagnetic exchange is rather weak ($-E_2/k$ =−2.16 K), corresponding to interactions (J=−3.00 cm^{-1}) within the Ising chain approximation ($\chi T \propto \exp[J/(2kT)]$).

From magnetic data of the above three compounds, it is clear that AF coupling mainly occurs between intrachain metal ions and obviously the antiferromagnetic coupling between intrachain metal ions is mediated by the hydrazine bridges. The magnetic coupling mechanism of hydrazine bridge is consistent with that of our previous work[4] which was examined using DFT+BS method.

3 Conclusions

To the best of our knowledge, it is the first time that compounds containing poly-hydrazine bridge have been synthesized and magnetically characterized. The X-ray crystallography analysis shows that two hydrazine molecules act as the bridge ligand forming the 1D chain compounds and 3D compound. The magnetic data reveal the overall AF magnetic coupling and the negative fitted values of J indicating intrachain interactions are AF coupling. This work is the complement of our previous work[4-5] and provides an unprecedented data for studying the coordination chemistry and magnetic properties of hydrazine compounds, and further enriches the field of molecule-based magnetic material.

Acknowledgments: We acknowledge the support of the National Natural Science Foundation of China (Grants No. 21101123, 21441007) and Department of Hubei Province (Grant No. D20131506). We also thank the Wuhan Institute of Technology (Grant No.CX2015160), supported by Graduate Innovative Fund of Wuhan Institute of Technology.

Supporting information is available at http://www.wjhxxb.cn

References:

[1] Xu H B, Wang Z M, Liu T, et al. *Inorg. Chem.*, **2007**,**46**: 3089-3096
[2] Armentano D, De Munno G, Mastropietro T F, et al. *Chem. Commun.*, **2004**:1160-1161
[3] Wang X T, Wang Z M, Gao S. *Inorg. Chem.*, **2007**,**46**: 10452-10454
[4] Jia L H, Li R Y, Duan Z M, et al. *Inorg. Chem.*, **2011**,**50**: 144-154
[5] WANG Yan-Jun(王艳君), JIA Li-Hui(贾丽慧), WANG Bing-Wu(王炳武). *Acta Phys. -Chim. Sin.*(物理化学学报), **2013**,**29**:701-705
[6] Blessing R H. *Acta Crystallogr. Sect. A*, **1995**,**51**:33-38
[7] Blessing R H. *J. Appl. Crystallogr.*, **1997**,**30**:421-426
[8] Sheldrick G M. *SHELXS*-97, *Program for Solution of Crystak Structures*, University of Göttingen, Germany, **1997**.
[9] Sheldrick G M. *SHELXL*-97, *Program for Refinement of Crystal Structures*, University of Göttingen, Germany, **1997**.
[10]Carlin R L. *Magnetochemistry*. Berlin: Springer-Verlag, **1986**: 2-3
[11]Feng S, Xu R. *Acc. Chem. Res.*, **2001**,**34**:239-247
[12]Zhang X M. *Coord. Chem. Rev.*, **2005**,**249**:1201-1219
[13]Heaton B T, Jacob C, Page P. *Coord. Chem. Rev.*, **1996**, **154**:193-229
[14](a) Harmony M D, Laurie V W. *J. Phys. Chem.*, **1979**,**8**:619-721
(b) Johnson R C. *Introductory Descriptive Chemistry*. New York: W. A. Benjamin Inc., **1966**:68
[15](a) Barrado G, Miguel D, Riera V, et al. *J. Organomet. Chem.*, **1995**,**489**:129-135
(b) Mosier P E, Kim C G, Coucouvanis D. *Inorg. Chem.*, **1993**,**32**:2620-3621
(c) Sellmann D, Kreutzer P, Huttner G, et al. *Z. Naturforsch. B*, **1978**,**33**,1341-1347
[16]Bourdreaux E A, Mulay L N. *Theory and Application of Molecular Magnetism*. New York: Wiley, **1976**.
[17](a) Wang X Y, Wei H Y, Wang Z M, et al. *Inorg. Chem.*, **2005**,**44**:572-583
(b) Sun H L, Wang Z M, Gao S. *Inorg. Chem.*, **2005**,**44**: 2169-2176
(c) Yang B P, Prosvirin A V, Guo Y Q, et al. *Inorg. Chem.*, **2008**,**47**:1453-1459
[18]Kahn O. *Molecular Magnetism*. New York: VCH, **1993**.
[19]Fisher M E. *Am. J. Phys.*, **1964**,**32**:343-346
[20](a) Liu T F, Fu D, Gao S. *J. Am. Chem. Soc.*, **2003**,**125**: 13976-13977
(b) Sun H L, Wang Z M, Gao S. *Chem. Eur. J.*, **2009**,**15**: 1757-1764
[21]Weng W. *Thesis for the Doctorate of Carnegie Institute of Technology*. **1968**.
[22]Rabu P, Rueff J M, Huang Z L, et al. *Polyhedron*. **2001**,**20**: 1677-1685